

SCIENTIFIC PAPERS  
OF THE UNIVERSITY OF PARDUBICE  
Series A  
Faculty of Chemical Technology  
22 (2016)

**MODELLING OF FLUIDIZED BED CHANNELLING  
USING A TWO-ZONE MODEL**

Ivam MACHAČ<sup>1</sup>, Bedřich ŠIŠKA, and Miloslav SIMON  
Institute of Environmental and Chemical Engineering,  
The University of Pardubice, CZ–532 10 Pardubice

Received May 2, 2016

This paper deals with the study of the structure of spherical particle beds fluidized with non-Newtonian aqueous polymer solutions in the creeping flow region in a two-dimensional rectangular column. It was confirmed that in fluidization with viscoelastic polymer solutions the bed channelling occurs and bed expansion reduces. A simple two-zone model was used to describe the bed channeling.

### **Introduction**

The fluidization of monodispersed beds of solid particles with liquids is usually considered to be uniform. However, extensive investigations of expansion of beds of solid particles fluidized with different kinds of non-Newtonian liquids performed in our laboratory have shown that the expansion course depends largely on the measure of rheological behaviour of the fluid [1-5]. For the fluidization with viscoelastic (pseudoplastic and simultaneously elastic) polymer solutions in

---

<sup>1</sup> To whom correspondence should be addressed.

creeping flow region, it has been observed that the fluidization becomes aggregative. The remarkable local particle concentration inhomogeneity gradually forms in the bed up to the state of bed channelling [6]. At the same time, the bed expansion is reduced due to that phenomenon.

It has been found that the shapes of expansion curves obtained for fluidization in cylindrical and narrow rectangular (“two-dimensional”) columns are similar [2]. From this, one can deduce that the structure of beds fluidized in these columns will be similar as well. At the same time, the formation of particle aggregates and the bed channelling occurring inside is visually observable in the “two-dimensional” column.

In this paper, the results are presented of examining the effect of the liquid rheological behaviour on the fluidized bed structure and expansion course in the flow of purely viscous and viscoelastic polymer solutions in the narrow rectangular column. The two-zone model was used to describe the fluidized bed channelling observed. The parameters of the two-zone model were evaluated using an image analysis of the video records of the flow through the bed.

For visualisation of the liquid flow, a method based on the observation of hydrogen bubbles released by electrolytic reduction of water was used.

## Two-Zone Model

The quantities characterizing the channelling process in a fluidized bed can be evaluated using the two-zone bed model [7]. The fluidized bed is considered to be divided into two zones: one with uniformly dispersed particles with the voidage  $\epsilon_1$  and the other consisting of a fluid channel (see Fig. 1). Then, the mean bed voidage is expressed as

$$\epsilon = \frac{V_{ch} + (V - V_{ch})\epsilon_1}{V} = \frac{S_{ch}}{S} + \left(1 - \frac{S_{ch}}{S}\right)\epsilon_1 = f \frac{u}{u_{ch}} + \left(1 - f \frac{u}{u_{ch}}\right)\epsilon_1 \quad (1)$$

where  $S$  is the cross-section of the whole bed,  $S_{ch}$  the cross-section of the channels,  $u$  the fluid superficial velocity,  $u_{ch}$  representing the velocity of the liquid flowing through the channels and

$$f = \frac{S_{ch}u_{ch}}{Su} \quad (2)$$

is the fraction of the liquid volume flow rate running through the channels.

If it is supposed that the voidage  $\epsilon_1$  is expressed by the Richardson-Zaki equation

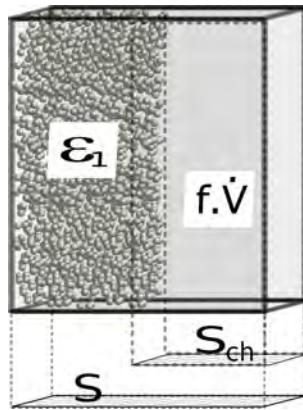


Fig. 1 Fluidized bed two-zone model

$$\varepsilon_1 = \left( \frac{u_1}{F_w u_t} \right)^{\frac{1}{z}} \quad (3)$$

where  $u_1$  is the superficial velocity of the liquid flowing through the particle zone,  $u_t$  the terminal falling velocity of particles,  $z$  the Richardson–Zaki exponent, and  $F_w$  is the wall factor, we can derive the following formula

$$f = 1 - \frac{1 - \varepsilon}{1 - \varepsilon_1} \varepsilon_1^z \frac{u_t}{u} F_w \quad (4)$$

The parameters needed for the model evaluation should be determined experimentally.

## Experimental

The extensive fluidization experiments were performed in the frame of the doctoral work [8]. Here, with respect to the limited extent of this contribution, only a representative set of experiments is presented.

The particle beds were composed from uniform glass spheres with a diameter and density specified in Table I. The test liquids were the aqueous solutions of methyl hydroxyethyl cellulose (called *Tylose*), hydroxyethyl cellulose (*Natrosol*), and polyacrylamides (*Praestol* and *Hercofloc*). Flow curves and creep and recovery tests of the liquids were measured with a rotational rheometer (model RheoStress RS 150) at ambient temperature (23 °C). The terminal velocities  $u_t$  of single particles in the test liquids were measured in a cylindrical Perspex tube (with 40 mm in diameter). A rectangular column made from transparent Perspex sheets was used for all fluidization experiments. The column cross-section dimensions were 5 mm × 80 mm and the height of the column was 800 mm. The

liquid was pumped by a gear pump, whereas volumetric liquid flow rate was controlled by changing the pump revolutions.

Table I Characteristics of the glass spheres used

Symbol	Diameter mm	Density $\text{kg m}^{-3}$
P1	4.12	2594
P2	3.47	2811

The hydrogen bubble visualization of the flow was based on the tracing of the gas released by electrolysis of water under a distribution unit carrying the bed of particles. The individual stages of fluidized bed expansion were recorded by a video camera and subsequently evaluated by means of the image analysis. The video sequences recorded by miniDV camera (model Canon M250i, Japan) were transferred into the computer through the interface (IEEE1394, FireWire). For the image processing and analysis, the freeware programs VirtualDub and ImageJ were used.

The layout of the experimental equipment is shown in Fig. 2. The measurements and the respective method of the result evaluation have been described in detail previously [8].

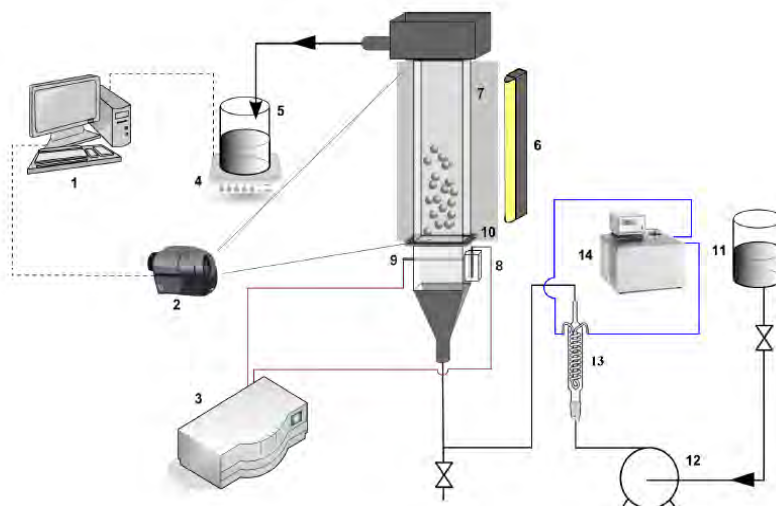


Fig. 2 Experimental setup: 1 – computer; 2 – video camera; 3 – DC power source; 4 – digital balance; 5 – collecting tank; 6 – fluorescent lamp; 7 – milk plexiglass; 8 – graphite anode; 9 – copper cathode; 10 – brass grid; 11 – liquid reservoir; 12 – gear pump; 13 – glass cooler; 14 – thermostat

## Results and Discussion

### Rheological Measurements

From the shear stress-shear rate data, the liquid viscosity functions and the parameters  $\eta_0$ ,  $\lambda$ , and  $m$  of the Carreau viscosity model

$$\eta = \frac{\eta_0}{[1 + (\lambda\dot{\gamma})^2]^{\frac{1-m}{2}}} \quad (5)$$

were determined; the liquid relaxation times

$$\lambda_c = \eta_0 J_s(t_0) \quad (6)$$

being evaluated from the creep and recovery tests. The viscosity functions obtained and the examples of creep and recovery tests are illustrated in Figs 3 and 4, respectively. The values of Carreau model parameters are given together with liquid densities and relaxation time in Table II. All the polymer solutions are shear thinning liquids.

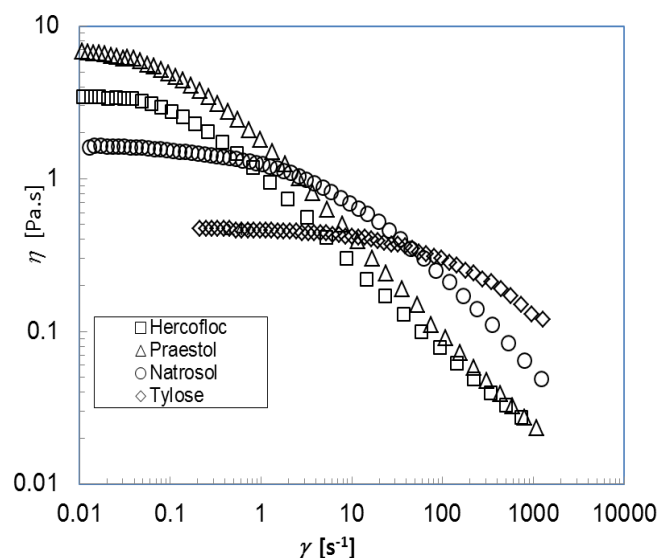


Fig. 3 Viscosity functions of polymer solutions used

The values of the relaxation time  $\lambda_c$  give evidence that the solutions of Tylose and Natrosol are very weakly elastic, whereas the solutions of Praestol and Hercofloc are strongly elastic; both in a linear meaning.

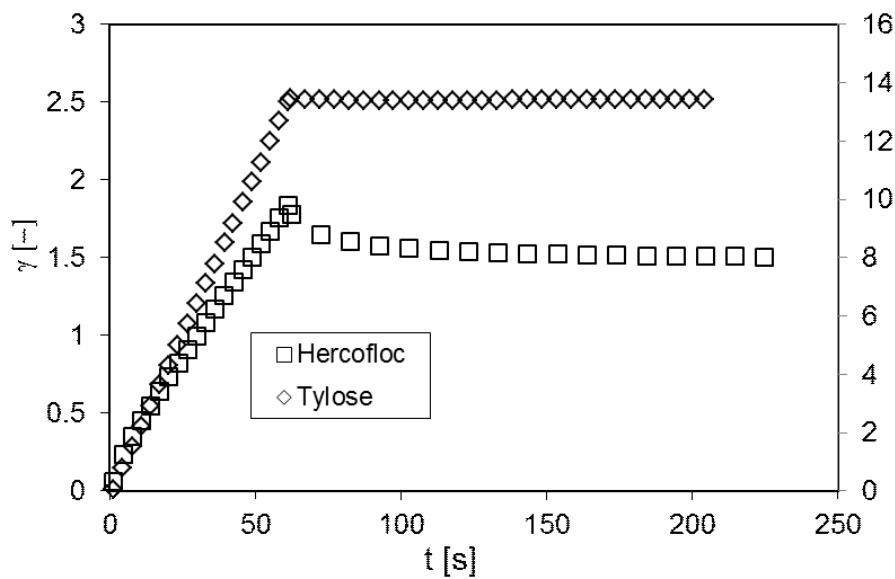


Fig. 4 Creep and recovery tests of polymer solutions used

Table II Characteristics of the test liquids (for 23 °C)

Symbol	Liquid	Concentration % wt.	Density kg m <sup>-3</sup>	Carreau model parameters			Rel. time
				$\eta_0$ , Pa s	$\lambda$ , s	$m$	$\lambda_{c2}$ , s
L1	Tylose	1.6	1003	0.448	0.041	0.687	0.629
L2	Natrosol	0.8	1002	1.477	0.496	0.496	1.85
L3	Praestol	0.6	1002	6.69	10.011	0.39	13.6
L4	Hercofloc	0.5	1001	3.511	14.388	0.444	9.34

### Expansion and Fluidized Beds Structure

Examples of dependences of the dimensionless velocity  $u_B = u/u_t$  upon the bed voidage  $\varepsilon$  (expansion curves) for fluidization of particles P1 with polymer solution used are shown in Fig. 5. Nearly the same course of expansion curves was observed for the fluidization of particles P2. It is evident that the bed expansion decreases with the increasing liquid rate, liquid shear thinning, and elasticity. This is due to the gradual loss of stability of the particulate fluidization; this process becoming aggregative, the particle chaining and bed channelling having manifested itself. This phenomenon is apparently evocated by the liquid linear elasticity (memory) and being enhanced by the formation of the liquid streams with lower viscosity due to the liquid shear thinning.

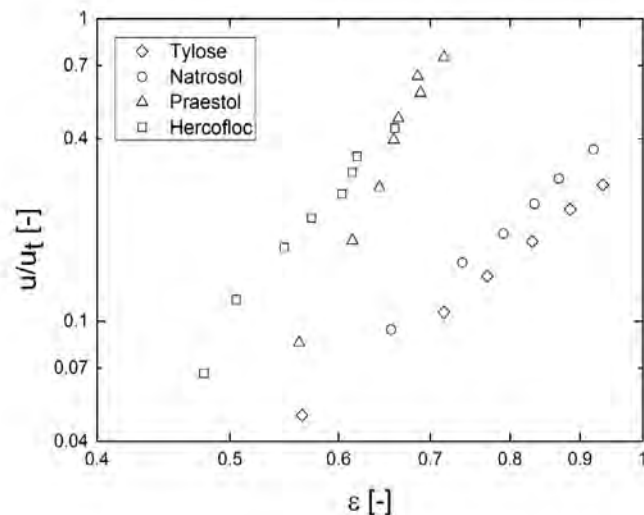


Fig. 5 Expansion curves for fluidization of particles P1 with polymer solutions used

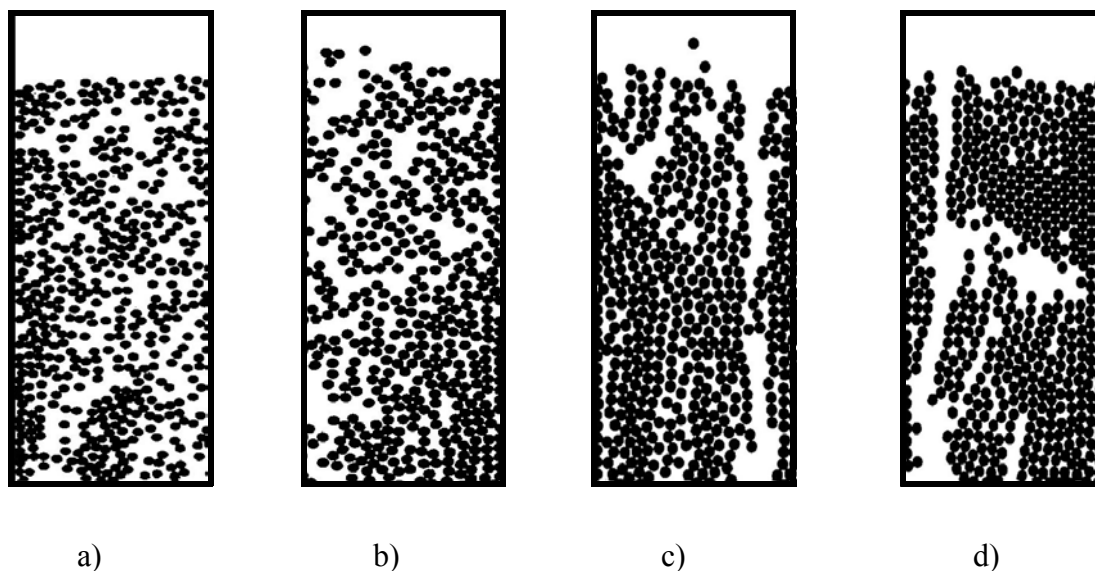


Fig. 6 Structure of particle P1 beds fluidized with liquids of different rheology: a – Tylose  $u_B = 0.142$ ,  $\varepsilon = 0.770$ ; b – Natrosol  $u_B = 0.157$ ,  $\varepsilon = 0.739$ ; c – Praestol  $u_B = 0.278$ ,  $\varepsilon = 0.643$ ; d – Hercofloc  $u_B = 0.312$ ,  $\varepsilon = 0.614$

Examples of structures of beds of spherical particles P1 fluidized with liquids differing by their shear thinning and linear elasticity are shown in Fig. 6. During fluidization with shear thinning and slightly elastic solutions of Tylose and Natrosol, only random aggregates of particles and similarly unconsolidated short channels are created. In the case of fluidization with the strongly shear thinning and elastic solutions of Praestol and Hercofloc, a few stable channels are formed, giving rise to a negligible bed expansion.

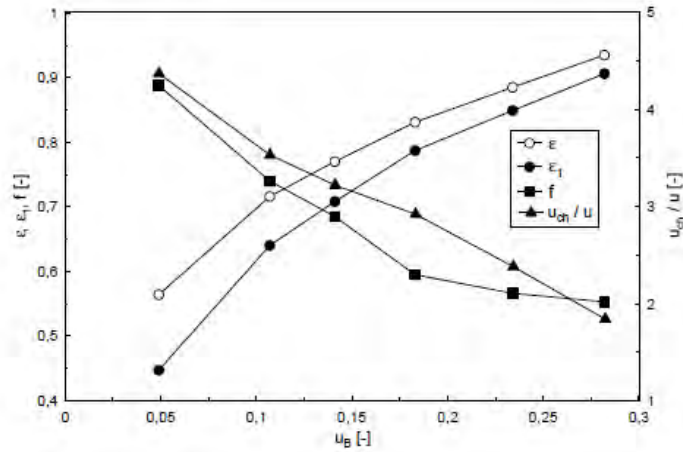


Fig. 7 Dependences of quantities  $f$ ,  $\epsilon_1$ ,  $\epsilon$ , and  $u_{ch}/u$  on  $u_B$  for system particle P1– solution of Tylose

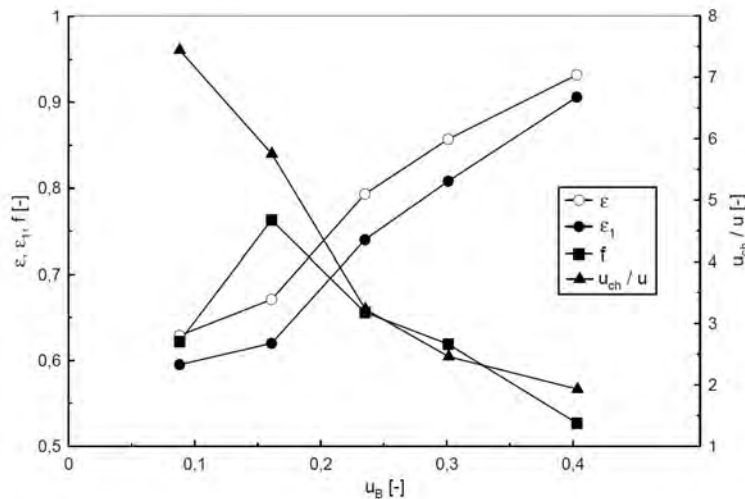


Fig. 8 Dependences of quantities  $f$ ,  $\epsilon_1$ ,  $\epsilon$ , and  $u_{ch}/u$  on  $u_B$  for system particle P2–solution of Natrosol

## Zone Model Evaluation

For this purpose, it was necessary to set the following variables:  $u$ ,  $u_p$ ,  $S_{ch}/S$ ,  $\epsilon$ ,  $z$ , and  $F_w$ . Values of variables  $u$  and  $\epsilon$  were obtained from the measurements of bed expansions, the values of variables  $u_t$  and  $F_w$  from the measurements of the terminal falling velocities of particles, and  $z = 4.71$  for the spherical particle bed fluidization in the creeping flow region [4]. The values of the ratio  $S_{ch}/S$  were determined by the image analysis applied to the corresponding fluidization video sequences. By knowing the values of the ratio  $S_{ch}/S$ , the values of the remaining variables  $\epsilon_1$ ,  $f$ ,  $u_{ch}$ , and  $u_1$  were calculated using the zone model equations (1), (4), (3), and (2).

Examples of the results obtained from the zone model for the individual systems tested are shown in a set of Figs 7-10. The results illustrate the analogous



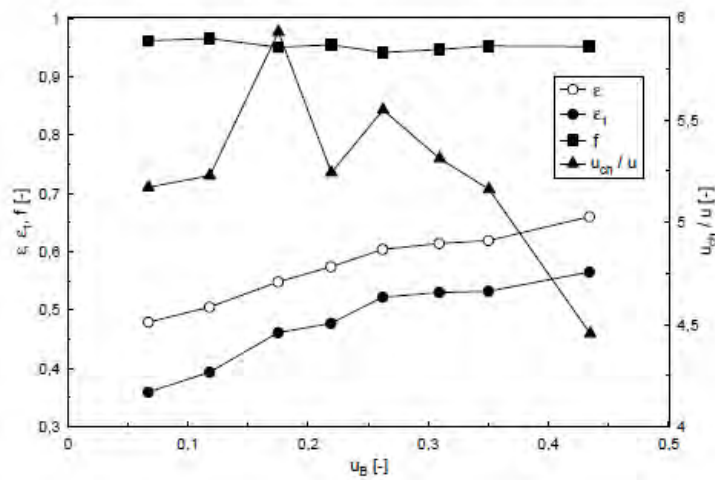


Fig. 9 Dependences of quantities  $f$ ,  $\varepsilon_1$ ,  $\varepsilon$ , and  $u_{ch}/u$  on  $u_B$  for system particle P1-solution of Hercofloc

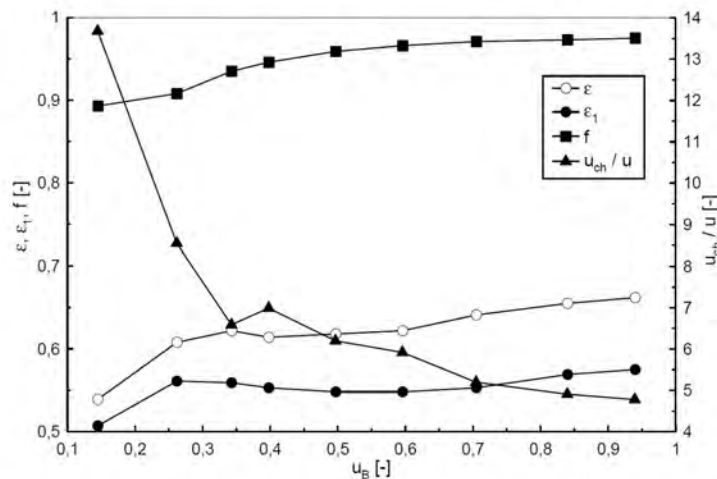


Fig. 10 Dependences of quantities  $f$ ,  $\varepsilon_1$ ,  $\varepsilon$ , and  $u_{ch}/u$  on  $u_B$  for system particle P2-solution of Praestol

course of fluidization by liquids with comparable rheological properties. During fluidization of particles P1 and P2 with the strong pseudoplastic and linearly elastic polymer solutions Praestol and Hercofloc, the fraction of the liquid volume flowing through the channels,  $f$ , is higher than 0.85 and the ratio  $u_{ch}/u$  is higher than 4.4. For fluidization with the polymeric solutions of Tylose and Natrosol, exhibiting only a weak linear elasticity, the values of the fraction  $f$  and the ratio  $u_{ch}/u$  are lower than those obtained for the solutions of Praestol and Hercofloc. This is in accordance with the lower degree of bed channelling observed. The velocities  $u_{ch}$  calculated using the zone model have been compared with those determined from the visualisation experiments, when the velocity of hydrogen bubbles carried by the liquid flowing in the channels had been measured. The maximal relative deviation between the calculated and experimental values of  $u_{ch}/u$  was 13.2 %, documenting applicability of the two-zone model to the description of the fluidized beds channelling.

## Conclusion

The expansion of spherical particle beds with liquids of different rheological behavior in rectangular columns was investigated by means of a flow visualization technique and an image analysis of the fluidized bed video-records.

It has been documented that the state of particulate fluidization, observed for fluidization with Newtonian liquids, changes to an aggregative status up to the channel formation in the case of fluidization with viscoelastic polymer solutions. The fluidized bed non-homogeneties and the channelling are growing with the increasing shear thinning and linear elasticity of the liquid.

A simple two-zone fluidized bed model has been applied to the description of bed channeling. In the case of fluidization with the strongly linearly elastic liquids, the high values of the fraction  $f$  show that the main part of liquid passes through the channels. Thus, it can be concluded that the fluidized bed apparatus are unsuitable for contacting the solid particles with these liquids in the creeping flow region (e.g. for heterogeneous catalysis or bioreactors).

## Symbols

$d$	particle diameter, m
$f$	fraction of the fluid volume flow rate flowing through the bed channels
$F_w$	corrective wall effect factor
$J_s$	steady state compliance, Pa <sup>-1</sup>
$m$	Carreau flow model parameter
$S$	fluidized bed cross-section, m <sup>2</sup>
$S_{ch}$	channel zone cross-section, m <sup>2</sup>
$u$	superficial velocity, m s <sup>-1</sup>
$u_B$	dimensionless superficial velocity
$u_{ch}$	mean velocity inside channel, m s <sup>-1</sup>
$u_t$	particle terminal falling velocity in an unbounded liquid, m s <sup>-1</sup>
$u_1$	superficial velocity related to the cross-section of the zone with particles, m s <sup>-1</sup>
$V$	fluidized bed volume, m <sup>3</sup>
$V_{ch}$	volume of channels in fluidized bed, m <sup>3</sup>
$\dot{V}$	volume flow rate, m <sup>3</sup> s <sup>-1</sup>
$z$	Richardson–Zaki exponent
$\dot{\gamma}$	shear rate, s <sup>-1</sup>
$\varepsilon$	mean bed voidage
$\varepsilon_1$	mean bed voidage of zone with particles
$\eta$	viscosity, Pa s
$\eta_0$	zero shear viscosity, Pa s
$\lambda$	Carreau flow model parameter, s

## References

- [1] Machač I., Mikulášek P., Ulbrichová I.: Chem. Eng. Sci. **48**, 2109 (1993).
- [2] Machač I., Šiška B., Lecjaks Z., Bena J.: Chem. Eng. Sci. **52**, 3409 (1997).
- [3] Machač I., Šiška B., Lecjaks Z.: Chem. Papers **53**, 390 (1999).
- [4] Teichman R., Brokl P., Šiška B., Machač I.: 15<sup>th</sup> International Congress CHISA, Prague, (2002).
- [5] Machač I., Comiti J., Brokl P., Šiška B.: TransICChemE **81**, Part A, 1217 (2003).
- [6] Šiška B., Doleček P., Bendová H., Machač I.: 16<sup>th</sup> International Congress CHISA, Prague, (2004).
- [7] Richardson J.F.: *Fluidization* (Davidson, J.F. and Harrison, D., Eds.), 25, Academic Press, New York, 1971.
- [8] Simon M.: *Study of Influence of Liquid Rheological Behavior on the Structure of Fluidized Beds of Spherical Particles* (in Czech), PhD thesis, University of Pardubice, 2014.